SUBMITTED MANUSCRIPT
JOURNAL SOLID STATE CHEMISTRY

On the boron rich phases in the Yb-B system

Oksana Sologub[a,*], Leonid P. Salamakha[a], Berthold Stöger[b], Peter F. Rogl[c], Takao Mori[d], Gaku Eguchi[a], Herwig Michor[a], Ernst Bauer[a]

[a]*Institute of Solid State Physics, TU Wien, A-1040 Wien, Austria*
[b]*X-Ray Centre, TU Wien, A-1060 Vienna, Austria*
[c]*Institute of Materials Chemistry and Research, University of Vienna, A-1090 Vienna, Austria*
[d]*National Institute for Materials Science, MANA, Namiki 1-1, Tsukuba, 305-0044, Japan*

ABSTRACT

Two boron rich phases were successfully synthesized by borothermal reduction of Yb oxide under vacuum. For the new boron-poorer phase, the single phase was established at around [B]/[Yb]=43.3 at 1500 °C (*Pbam* space group; YB_{50}-type; a=16.5811(5) Å, b=17.5950(5) Å, c=9.4647(3) Å; powder X-ray diffraction; Rietveld refinement). The crystal structure of the boron-richer phase ([B]/[Yb]=56.0) has been elucidated by single crystal X-ray diffraction ($Fm\bar{3}c$ space group; YB_{66}-type; a=23.3587(6) Å). Powder X-ray diffraction data of the alloy $YbB_{\sim 70}$ annealed at 1825 °C yielded, along with the YB_{66}-type compound (a=23.3691(2) Å), *β-rh* B as a secondary phase ($R\bar{3}m$ space group, a=10.9298(3) Å, c=23.875(1) Å), for which the solubility of Yb was found to be below 1 at.%. Both $YbB_{43.3}$ and $YbB_{56.0}$ feature complicated boron atom frameworks which exhibit shorter B-B separations both within and between boron clusters as compared to those observed for prototype structures.

Keywords: Rare-earth borides; boron icosahedral framework; crystal structure; X-ray diffraction

* Corresponding author.
E-mail address: oksana.sologub@univie.ac.at (O. Sologub).

1. Introduction

A number of binary phases displaying icosahedral boron frameworks have been reported to exist in the Y(RE)-B systems when RE is a heavier rare earth element, among them the compounds with yttrium were studied most explicitily. The yttrium borides richest in boron (YB_{66}-type structure, $Fm\bar{3}c$ space group) [1-3] have been repeatedly examined due to their desirable properties for application as high-resolution and synchrotron-radiation-resistant monochromators [4-6]. The complicated structure of YB_{66} is constructed of eight $[B_{12}]_{13}$ supericosahedra and eight B_{80} clusters centered in 8*a* (¼,¼,¼); the non-icosahedral borons are distributed in four partially occupied crystallographic positions (3×192*j*; 1×64*g*) (Fig. 1). The partially filled Y sites (48*f*) octahedrally enclose the B_{80} cluster; the coordination spheres of ytrium atoms include as well the twelve surrounding icosahedral borons. YB_{66} crystallizes in a significantly wide homogeneity range from YB_{56} to $YB_{\sim 70}$ as estimated by single crystal X-ray diffraction (XRD) and chemical analyses [6,7]; a much more metal-rich composition, YB_{48}, as a consequence of partial Y population of the 8*a* site inside the B_{80} cluster has been reported recently [8]. The compounds exhibiting the YB_{66}-type boron atom skeleton were reported to occur in the boride systems with Pr-Sm, Gd-Lu, Th and Pu [9-11]. They are extremely hard with microhardness values ranging from about 3600 to 4000 kp/mm^2 [12] and 2300±50 to 2620±50 kp/mm^2 [9] according to different literature sources and melt at ~2150±100ºC (as measured for Nd, Sm, Gd, Dy, Er and Yb borides [12]).These compounds are also of interest as short range magnetic transitions [13] and spin glass behavior [14] were claimed at low temperatures. The YB_{66}-type compounds are p-type thermoelectric materials [15], with a marked enhancement of the thermoelectric figure of merit recently reported for SmB_{62} [16].

In the course of YB_{66} single crystal growth studies, Tanaka et al. [17] discovered two more previously unknown boron-rich compounds. The higher boron content phase formed as single phase at a nominal composition B/Y=50, while at mixing ratios of B/Y=25.5-26.0, a phase with a a different structure type was observed. Because of the unavailability of single crystals, the crystal structure of YB_{50} was elucidated from powder XRD and electron diffraction analysis as orthorhombic with lattice constants a=16.6251 Å, b=17.6198 Å and c=9.4797 Å; detailed structure analysis has been carried out from single crystal studies of the isotypic Si-containing phase [18]. Silicon atoms were found to statistically share certain atom positions in the $[B_{12}Si_{1.5}B_{1.5}]$ unit with boron. Beside the 15-atoms cluster, the boron atom framework is composed of five crystallographically different $[B_{12}]$ icosahedra and several

interstitial bridging sites displaying various occupancies. In contrast to other boron-rich borides, the Y site in this structure is fully occupied, thus the reported varieties of chemical compositions result from differences in the boron atom site occupancies. YB_{50} exists in a limited temperature range; at 1700 ºC it starts to decompose into YB_{25} and YB_{66} [19]. The YB_{50} isotypic compounds were mentioned to form with rare earth elements from Tb to Lu [17]. The third compound at the boron rich end of the Y-B system, YB_{25}, is stable up to 1850 ºC; at higher temperatures it decomposes to YB_{12} and YB_{66}. The crystal structure-type of this phase was first elucidated for TbB_{25} from powder diffraction [20], and consistent with later results from a carbon containing single crystal [21]; the compound is structurally related to $MgAlB_{14}$ [22] with an empty Al site and Y atoms occupying the Mg sites (*C*2/*m* space group a=10.1038 Å, b=10.327 Å, c=5.86 Å).

In contrast to yttrium borides, the situation regarding higher borides in the Yb-B system is not well defined [23,24]. Schwetz et al. [9] reported lattice parameters (space group $Fm\bar{3}c$, a=23.422(3) Å) and microhardness (2410±50 kp/mm^2) for the YbB_{66} obtained by arc-melting a [B]/[Yb]=12 mixture; the resulting two-phase alloy contains boron as additional phase. Spear and Solovyev [12] synthesized by arc melting mixtures of the elements single-phase YbB_{66} which exhibits smaller lattice parameters (a=23.415 Å) and a higher value of microhardness (2960±200 kp/mm^2). In both cases, the identification of phases and the evaluation of lattice parameters have been performed exclusively by powder XRD techniques; moreover neither the metal to boron ratio of this class of ytterbium borides nor upper and lower composition limits and their temperature dependence have yet been established. Mori [25] evaluated lattice parameters and studied magnetic properties of the silicon doped YB_{50}-type ytterbium boride (*Pbam* space group, a=16.636(4) Å , b=17.644(2) Å, c=9.488(2) Å) from a sample grown by the floating zone method, however, no data on composition and structure exist in the literature for the binary ytterbium boride. In our current work we evaluated the composition range and investigated the crystal structure of YB_{66}-type ytterbium boride in more detail both from single crystal and powder XRD. Futhermore, we synthesized for the first time a new binary ytterbium boride of YB_{50}-type in single phase condition and report its structural parameters as well as we clarified the atom site preferences of Yb in the *β-rh* boron stucture at ~0.72 at.% doping level at 1825 °C from the sample at the boron-rich boundary of the YB_{66}-type ytterbium boride.

2. Experimental

2.1. Synthesis

The proper weight ratios of amorphous boron (3N, SB-Boron Inc., USA) and ytterbium oxide (Yb_2O_3, 3N, Koujundo Kagaku Co., Japan) to obtain the $YbB_{\sim 50-\sim 70}$ compositions ($Yb_2O_3+(2m+3)B \rightarrow 2YbBm+3BO\uparrow$) were well mixed in mortars and compacted by cold iso-static pressing into cylindrical bars applying a pressure of 300 MPa. Each compacted rod was placed in a BN crucible inserted into a graphite susceptor. The reaction processes were performed under dynamic vacuum at a predetermined temperature of 1500 °C, 1675 °C and 1825 °C for 4 h each using a radio frequency (RF) induction furnace; afterwards the setup was cooled down in 1h to room temperature. Temperature was verified using an optical pyrometer by simulating black body condition through a small drilled hole in the crucible lid. The samples were crushed, reshaped, and subjected to a second anneal in order to attain homogeneity. The chemical analyses of samples synthesized by this method showed less than 0.1 wt.% of oxygen and carbon impurities.

2.2. Powder XRD

Powder XRD data were collected at room temperature using a Guinier-Huber image plate system with monochromatic Cu $K_{\alpha 1}$ radiation ($7^\circ<2\theta<100^\circ$) and a Siemens D5000 diffractometer with Cu Kα radiation ($5^\circ<2\theta<110^\circ$; step scan 0.02º; counting time per step 30 s). Phase analyses and structure refinements from powder XRD data were performed with the program FULLPROF [26] starting from the atomic positions obtained from the single crystal XRD studies presented in the current work ($YbB_{56.0}$) and reported recently for the Pt-doped YB_{50}-type structure [27].

2.3. Single crystal XRD

A single crystal was isolated from the fragmented melted portions of the sample $YbB_{\sim 70}$ annealed at 1825 °C. X-ray single crystal intensity data were collected on a Bruker APEX II diffractometer (CCD detector, κ-geometry, Mo Kα radiation). Orientation matrix and unit cell parameters were derived with the help of the program DENZO; multi-scan absorption correction was applied using the program SADABS; frame data were reduced to

intensity values applying the SAINT-Plus package [28,29]. The analysis of systematic absences was performed with the help of program ABSEN [30,31]. The structure was solved by direct methods (SHELXS-97 [32]) and refined with the program SHELXL-97 [33]. Atom coordinates were standardized with the program STRUCTURE TIDY [34]. Further details concerning the experiments are summarized in Table 1 and Table 2. Detailed description of structural refinement is given below.

3. Results and Discussion

3.1. Crystal structure of $YbB_{56.0}$

In agreement with the work of Richards and Kasper [2], structure solution with direct methods in the space group $Fm\bar{3}c$ resulted in one atom position (48*f*) exhibiting outstanding electron density peaks along with few atom sites ocupied by much lighter atoms; upon assigning 50% Yb occupancy to the 48*f* site, the 9 boron atom positions which build the icosahedral framework were easily obtained from difference Fourier synthesis. Additionally, 4 atom positions partially occupied by boron atoms were observed for the regions surrounding the Yb atoms in the structure. The refinement with free site occupation factors for Yb1 and B10-B14 applying the anisotropic ADP's for ytterbium and for fully occupied boron sites led to a reliability factor as low as R_F^2=0.075 and revealed a 3.1 el/Å^3 peak of electron density located at 0.6 Å from Yb1. Following the consideration of Tanaka et al. [35] for YB_{62}, a split Yb1/Yb11 atom position was introduced rendering a significant reduction of the residual factor; when allowed to refine freely, the occupancy of Yb1/Yb11 sites converged to 0.443/0.142. A final structure refinement yielded R_F^2=0.0442 and a residual electron density as low as 0.93 el/Å^3 (Table 1). The complicated structure model obtained from single crystal data was confirmed by Rietveld analysis of the X-ray powder data for the $YbB_{\sim 70}$ sample annealed at 1825 ºC (Fig. 2) exhibiting low residual values and good agreement between calculated and observed intensities.

The $YbB_{56.0}$ crystal structure (Fig. 1) can be described by fourteen independent atoms: one ytterbium and thirteen borons (Table 1). B1 to B9, whose sites are fully occupied, build a basic structural unit, the supericosahedron constructed of 12 outer icosahedra [$B2_1B3_1B4_1B5_1B6_2B7_2B8_2B9_2$]) grouped around the [$B1_{12}$] central one (Fig. 3a). The remaining B10 to B13 atoms form non-icosahedral cages which occupy statistically the voids within the icosahedral framework centered at the body center of the octants of the unit cell.

Comparing the atomic positions and bond lenghts of $YbB_{56.0}$ and YB_{62} [35], one can conclude that the boron framework of $YbB_{56.0}$ made up of $([B_{12}])_{13}$ "supericosahedra" is slightly compressed as compared to YB_{62}. A small shift of B2 along *y* delivered a rather short contact distance of 1.600 Å between B1 of the central icosahedron and B2 of surrounding ones (Fig. 3c). The outer icosahedra of $([B_{12}])_{13}$ are inter-linked via B3-B3 and B6-B8 bonds (Figs. 3d, 3b), among which the B3-B3 contact distance is slightly shorter from that in YB_{62} (1.804 Å vs 1.820 Å respectively). The central $[B1_{12}]$ icosahedron is smaller and more regular in $YbB_{56.0}$; two bond lenghts which define its edges (1.724 Å and 1.737 Å, Table 2) do not differ as much as in YB_{62} (1.729 Å and 1.768 Å). The $([B_{12}])_{13}$ units are inter-joined via two kinds of external bonds, B4-B5 and B7-B7; the contact distances between these atoms are comparable to those observed in YB_{62}. The remaining B9 atom of the $[B_{12}]$ outer icosahedron is not involved in the external bonding to other icosahedra; it builds, together with atom sites B4, B5 and B10, B11 and B12 partially occupied atom positions, the peanut shaped cage hosting the Yb atoms (Fig. 3e). Similarly to YB_{62}, the short Yb1-Yb11 and Yb1-Yb1 separation distances prevented the coexistence of all three atoms in the unit cell; according to refined occupancy parameters, about 44% of unit cells are statistically occupied by Yb1 (in 48*f*, *x*,¼,¼; -*x*, ¼,¼, *x*=0.0544) while 14% of unit cells are populated by Yb11 (in 48*f*, x=0.0726). The Yb1 and Yb11 bonds to B9, B4 and B5 icosahedral atoms exhibit lenghts (Table 2) comparable with those observed in YbB_{12} [36]. The B10-B13 unit consists of a set of three cages. The outer most cage includes B10 and B12, the middle one is formed by B11 and the inner cluster is constructed by B13. In agreement with the previous reports on YB_{66} [2,6,35], the number of atom sites involved in each cluster in $YbB_{56.0}$ is 80, however the actual number of boron atoms assigned to the individual cage is smaller due to partial occupancies. The thermal ellipsoids for the atoms which construct the cluster are considerably larger than those of the icosahedral sites, thus the calculated interatomic distances for these atoms should be interpreted only as indicating the long or short bonds (Table 2).

Table 1. X-ray single crystal data for $YbB_{56.0}$.

Formula from refinement	$Yb_{1.17}B_{65.84}$
Nominal composition	$Yb_{1.75}B_{98.25}$
Space group	$Fm\bar{3}c$ (No. 226)
Structure type	YB_{66}
Diffractometer	Bruker APEX II
Range for data collection (deg)	$3.02<\theta<27.93$
Crystal size	45x48x47 μm^3
a (Å) (single crystal)	23.3587(6)
Reflections in refinement	551 $F_o > 2\sigma(F_o)$ of 686
Mosaicity	<0.4
Number of variables	110
$R_F^2 = \Sigma\|F_0^2-F_c^2\|/\Sigma F_0^2$; GOF	0.0442; 1.122
Extinction (Zachariasen)	0.00002(2)
Residual density (el/Å^3)	0.93; -0.44
B1 in 96*i* (0,*y*,*z*); occ.; U_{iso} [a]	*y*=0.0372(3), *z*=0.0597(3); 1.00; 0.012(1)
B2 in 96*i* (0,*y*,*z*); occ.; U_{iso}	*y*=0.0750(3), *z*=0.1164(3); 1.00; 0.013(1)
B3 in 96*i* (0,*y*,*z*); occ.; U_{iso}	*y*=0.0386(3), *z*=0.1810(3); 1.00; 0.012(1)
B4 in 96*i* (0,*y*,*z*); occ.; U_{iso}	*y*=0.1487(2), *z*=0.2417(2); 1.00; 0.011(1)
B5 in 96*i* (0,*y*,*z*); occ.; U_{iso}	*y*=0.1858(2), *z*=0.1718(3); 1.00; 0.011(1)
B6 in 192*j* (*x*,*y*,*z*); occ.; U_{iso}	*x*=0.0391(2), *y*=0.1401(2), *z*=0.1220(2); 1.00; 0.014(1)
B7 in 192*j* (*x*,*y*,*z*); occ.; U_{iso}	*x*=0.0391(2), *y*=0.0819(2), *z*=0.2294(2); 1.00; 0.012(1)
B8 in 192*j* (*x*,*y*,*z*); occ.; U_{iso}	*x*=0.0625(2), *y*=0.0772(2), *z*=0.1589(2); 1.00; 0.012(1)
B9 in 192*j* (*x*,*y*,*z*); occ.; U_{iso}	*x*=0.0636(2), *y*=0.1457(2), *z*=0.1951(2); 1.00; 0.014(1)
B12 in 192*j* (*x*,*y*,*z*); occ.; U_{iso}	*x*=0.1289(7), *y*=0.1742(7), *z*=0.2426(9); 0.38(3); 0.042(7)
B10 in 192*j* (*x*,*y*,*z*); occ.; U_{iso}	*x*=0.1324(4), *y*=0.1744(4), *z*=0.1971(4); 0.79(3); 0.046(4)
B11 in 192*j* (*x*,*y*,*z*); occ.; U_{iso}	*x*=0.1608(5), *y*=0.2316(6), *z*=0.1979(6); 0.45(3); 0.037(5)
B13 in 64*g* (*x*,*x*,*x*); occ.; U_{iso}	*x*=0.2309(6); 0.31(3); 0.038(9)
Yb1 in 48*f* (*x*,¼,¼); occ.; U_{11},	*x*=0.0544(2); 0.443(11); 0.013(1),
$U_{22}=U_{33}$, $U_{23}=U_{13}=U_{13}=0$	0.0168(6)
Yb11 in 48*f* (*x*,¼,¼); occ.; U_{iso}	*x*=0.0726(6), 0.142(9); 0.055(3)

[a] isotropic (U_{iso}) and anisotropic (U_{ij}) atomic displacement parameters (Å^2)

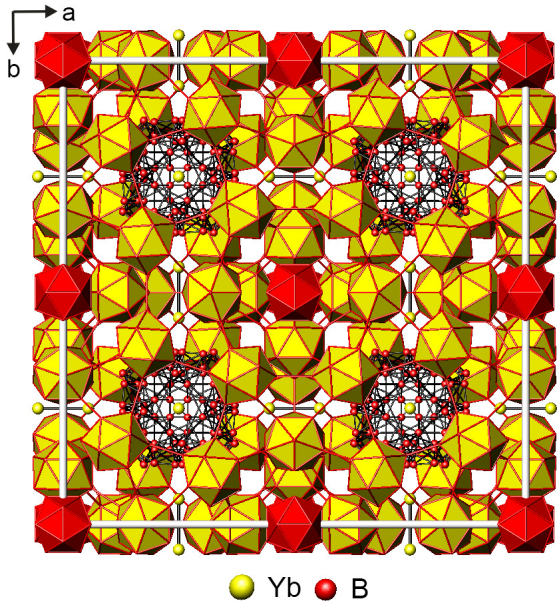

Fig. 1. Unit cell of $YbB_{56.0}$ (YB_{66}-type structure) as seen along the *c* axis ($-0.07 \leq z \leq 0.57$) showing the arrangement of twelve [B_{12}] icosahedra (yellow, in printed version - light grey) around the central one (red, in printed version - dark grey) along with Yb atoms and the clusters of 80 partially occupied boron sites. Yb in split atom position and Yb-B bonds are omitted.

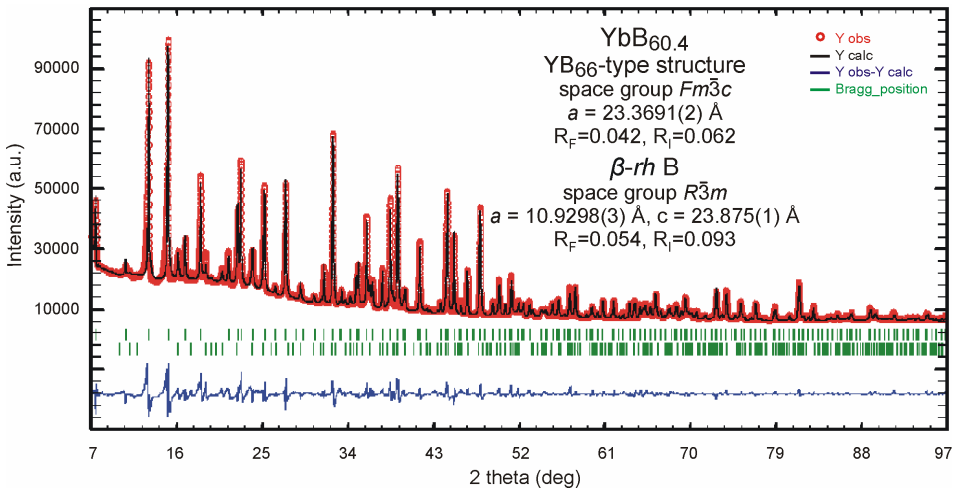

Fig. 2. Rietveld X-ray powder diffraction refinement of $YbB_{\sim 70}$ heat-treated at 1825 ºC, revealing the majority phase $YbB_{60.4}$ with YB_{66}-type structure (upper row). Occupancies of Yb1 and Yb11 were refined to 42.6% and 11.3% respectively. For *β-rh* B (lower raw), the best fit between observed and calculated intensities was achieved applying the structure model reported for Sc-doped *β-rh* B ($Sc_{1.61}B_{103}$ [37]). Occupancies of the Yb atom sites in *β-rh* B structure were obtained as follows: Yb in 6*c* (E) Occ. 29.2%; Yb in 18*h* (D) Occ. 2.8%; suggesting a total solubility of 0.72 at.% Yb. The A1 void (6*c*) was found to be unoccupied.

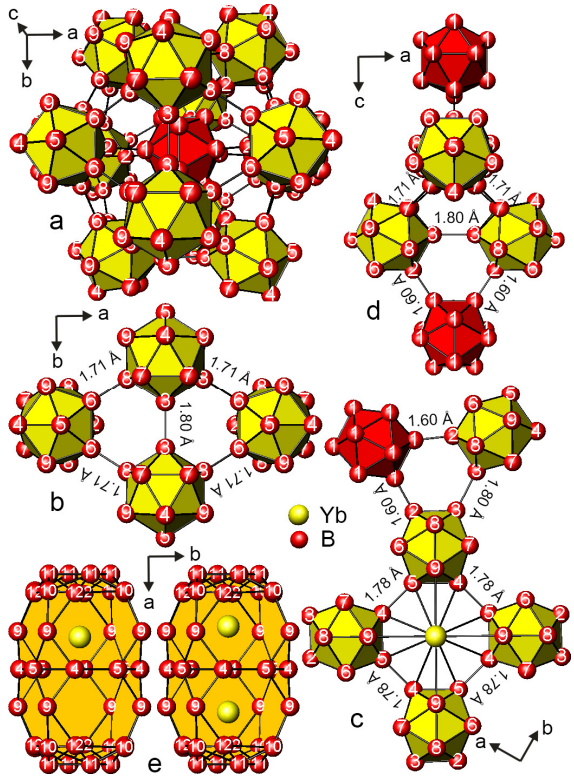

Fig. 3. Linkage of icosahedra (b-d) in $([B_{12}])_{13}$ unit (a) of the $YbB_{56.0}$ structure and two possible cases of Yb atom population of B cage (e). The atom labels correspond to the boron atom numbers in Tables 1-2.

3.2. Crystal structure of $YbB_{43.3}$

Similarly to yttrium boride, our $YbB_{\sim 50-\sim 60}$ samples, sintered and annealed at 1500 ºC, did not show any crystal specimens, suitable for single crystal X-ray diffraction studies. Careful examination of the X-ray powder diffraction pattern revealed similarities with the experimental diffractogram of YB_{50} reported previously [19,27] suggesting isotypism of these compounds. The results of indexing confirmed our expectation rendering an orthorhombic unit cell with a=16.58 Å, b=17.60 Å, c=9.46 Å. No additional reflections indicating the formation of secondary phases have been observed. Using atom coordinates derived from our recent single crystal X-ray diffraction study of Pt-doped silicon free YB_{50} boride [27] as the initial starting parameters for the refinement, we were able to satisfactorily refine the atomic positions of the ytterbium containing YB_{50}-type phase (Table 3). The final refinement led to the composition $YbB_{43.3}$ resulting in a perfect agreement between calculated and observed intensities (Fig. 4). The refined atom coordinates, isotropic displacement parameter for Yb1 and occupation factors for interstitial sites are listed in Table 3. The boron framework is

proven to be made up of five crystallographically different [B_{12}] icosahedra and the [B_{15}] unit (Fig. 5a). The apical atoms in the 15-boron atoms unit are linked to the surrounding fourteen [B_{12}] icosahedra and one [B_{15}]. The B-B distances between two [B_{15}] units in $YbB_{43.3}$ and Pt-doped YB_{50}-type boride are comparable (1.73 Å and 1.81 Å respectively), however, they are substantially shorter than the equivalent distance in the silicon-doped YB_{50} structure (about 2 Å) [18] where the linkage is realized via B-Si or B-B bonds. There is only one type of coordination environment of Yb (8*i* (*x*,*y*,*z*) *x*=0.1029(1), *y*=0.4485(1), *z*=0.2343); four ytterbium atoms are arranged to form a rectangle with side lenghts of 3.874 Å (in the *ab* plane) and 4.413 Å (along *c* direction) (Figs. 5b, 5c). Alike in Pt-doped YB_{50}-type boride [27], the subsequent shortest distance between ytterbium atoms in $YbB_{43.3}$ along *c* direction is 5.00 Å.

Table 2. Distances in $YbB_{56.0}$ (in Å)[a]

B1- B2 1.600(8)	B6-B8 1.707(5)	B9- B12 2.00(1)	B12- B10 2.02(2)
B1-4B1 1.724(7)	B6-B2 1.779(6)	B9- Yb11 2.762(4)	B12- Yb11 2.21(2)
B1- B1 1.737(9)	B6-B8 1.789(6)	or	or
	B6-B9 1.805(6)	B9- Yb1 2.762(4)	B12- Yb1 2.49(2)
B2- B1 1.600(8)	B6-B5 1.824(6)		
B2- B3 1.732(8)	B6-B6 1.827(8)	B10- B9 1.742(9)	B13- 3B11 1.81(2)
B2-2B8 1.767(5)		B10- B11 1.76(1)	B13- 2B11 2.01(1)
B2-2B6 1.779(7)	B7-B7 1.710(8)	B10- B11 1.87(1)	
	B7-B8 1.739(6)	B10-2B10 1.88(1)	Yb1- 4B12 2.49(1)
B3- B2 1.732(8)	B7-B3 1.770(7)	B10-2B12 2.01(2)	Yb1- Yb1 2.541(9)
B3-2B7 1.770(7)	B7-B9 1.786(6)	B10-Yb11 2.57(1)	Yb1- 4B5 2.684(5)
B3-2B8 1.792(6)	B7-B7 1.828(8)	or	Yb1- 4B4 2.692(5)
B3- B3 1.804(9)	B7-B4 1.832(6)	B10-Yb1 2.82(1)	Yb1- 4B9....2.762(4)
			Yb1- 4B11..2.80(1)
B4- B5 1.779(7)	B8-B6 1.707(5)	B11- B12 1.66(2)	Yb1- 4B10..2.82(1)
B4-2B7 1.832(6)	B8-B7 1.739(6)	B11- B10 1.76(1)	
B4-2B9 1.843(5)	B8-B2 1.767(5)	B11- B13 1.81(2)	Yb11-4B12 2.21(1)
B4- B5 1.847(7)	B8-B6 1.789(6)	B11-2B11 1.83(1)	Yb11-4B11 2.43(1)
B4-2Yb1 2.692(5)	B8-B3 1.792(6)	B11- B12 1.86(2)	Yb11-4B10 2.57(1)
or	B8-B9 1.810(6)	B11- B10 1.87(1)	Yb11-4B9....2.762(4)
B4-2Yb11 2.917(9)		B11- B13 2.01(1)	Yb11-4B5....2.91(1)
	B9-B10 1.742(9)	B11- B11 2.03(2)	Yb11-4B4....2.92(1)
B5- B4 1.779(7)	B9-B7 1.786(6)	B11-Yb11..2.43(1)	Yb11-Yb11..3.39(1)
B5-2B6 1.824(6)	B9-B6 1.805(6)	or	
B5-2B9 1.839(5)	B9-B8 1.810(6)	B11-Yb1 2.80(1)	
B5- B4 1.847(7)	B9-B5 1.839(5)		
B5-2Yb1 2.684(6)	B9-B4 1.843(5)	B12- B11 1.66(2)	
or		B12- B11 1.86(2)	
B5-2Yb11 2.909(9)		B12- B9 2.00(1)	
		B12- B10 2.01(2)	

[a]Short distances between atom sites which can not be simultaneously occupied are as follows: B10-B12: 1.07(2) Å, B10-B11: 1.49(1) Å, B11-B12: 1.11(2) Å, B11-B11: 1.49(2) Å, B12-B12: 1.53(3) Å, B13-3B13: 0.89(3) Å, B13-3B13: 1.26(4) Å, B13-B13: 1.54(5) Å.

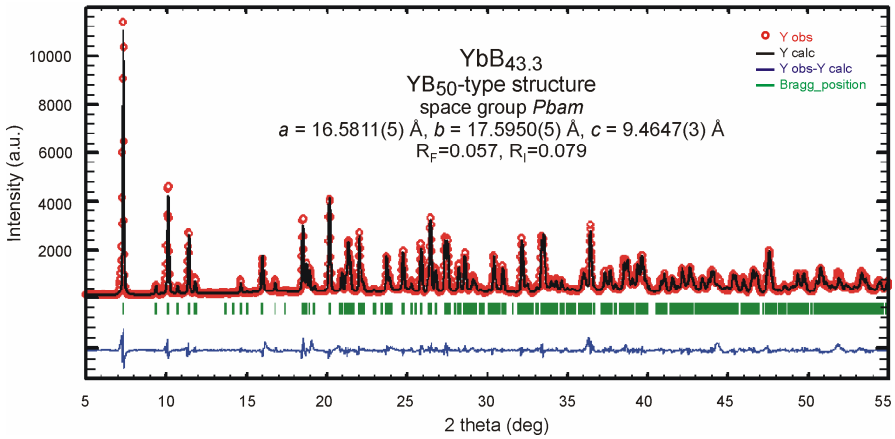

Fig. 4. Rietveld X-ray powder diffraction refinement of sample $YbB_{\sim 60}$ heat-treated at 1500 ºC, revealing single-phase $YbB_{43.3}$ with YB_{50}-type structure. Subsequent annealing at 1675 ºC drastically reduced the amount of the YB_{50}-type phase and yielded a substantial amount of the YB_{66}-type high-temperature phase (space group $Fm\bar{3}c$, a=23.3799(2) Å; Occ. Yb1 42.2%, Occ. Yb11 12.5%) along with a minor quantity of an unknown phase.

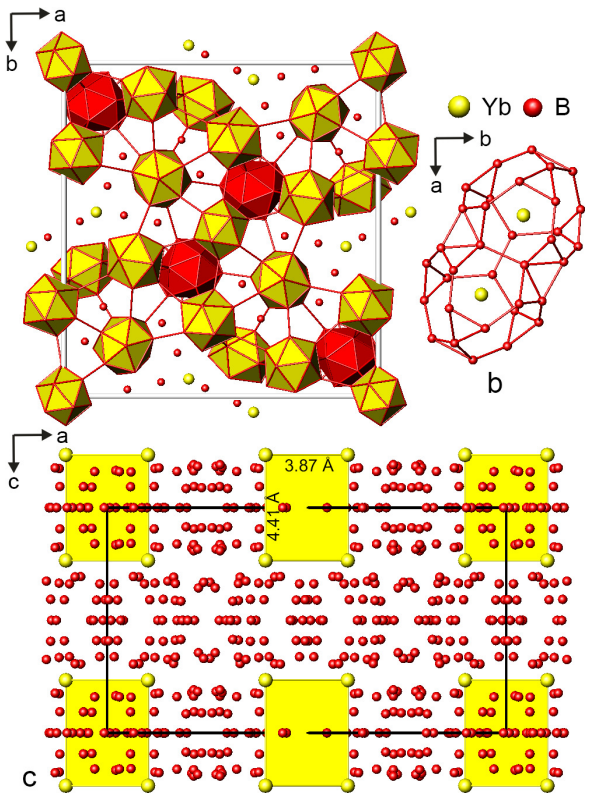

Fig. 5. Polyhedral view of the $YbB_{43.3}$ structure displaying boron icosahedra (yellow, in printed version - light grey) and 15-boron atom units (red, in printed version - dark grey) (a). Atom coordination around Yb1 ($d_{Yb1\text{-}Yb1}$=3.874 Å) (b). Crystal structure of $YbB_{43.3}$ along the *b*-axis emphasizing the arrangement of ytterbium atoms and nearest Yb1-Yb1 separation distances (c).

Table 3. Atomic coordinates for $YbB_{43.3}$[a] (*Pbam* space group (No. 55), YB_{50}-type structure, a=16.5811(5) Å, b=17.5950(5) Å, c=9.4647(3) Å, R_F=0.057, R_I=0.079, 701 reflections).

Atom	Site	*x*	*y*	*z*
Yb1	8*i*	0.1029(1)	0.4485(1)	0.2343(2)
B2	8*i*	0.031(2)	0.037(3)	0.160(3)
B27	8*i*	0.441(2)	0.450(3)	0.093(3)
B43	4*g*	0.007(3)	0.091(3)	0
B47	4*g*	0.087(3)	0.029(3)	0
B12	8*i*	0.217(2)	0.104(3)	0.163(3)
B15	8*i*	0.263(2)	0.012(2)	0.089(3)
B17	8*i*	0.282(2)	0.178(2)	0.094(3)
B20	8*i*	0.325(2)	0.089(2)	0.161(3)
B50	4*g*	0.182(3)	0.052(3)	0
B51	4*g*	0.200(3)	0.159[b]	0
B52	4*g*	0.355(3)	0.030(3)	0
B53	4*g*	0.360(3)	0.138(3)	0
B1	8*i*	0.022(2)	0.315(2)	0.165(3)
B3	8*i*	0.061(2)	0.228(2)	0.159(3)
B6	8*i*	0.118(2)	0.309(2)	0.094(3)
B28	8*i*	0.462(2)	0.266(2)	0.091(3)
B44	4*g*	0.022(3)	0.180(3)	0
B46	4*g*	0.060(3)	0.365(3)	0
B49	4*g*	0.127(3)	0.219(3)	0
B54	4*g*	0.454(3)	0.180[b]	
B24	8*i*	0.380(2)	0.097(2)	0.335(3)
B25	8*i*	0.393(3)	0.195(2)	0.409(3)
B29	8*i*	0.474(2)	0.054(2)	0.410(3)
B30	8*i*	0.482(2)	0.150(2)	0.338(3)
B33	4*h*	0.040(3)	0.380(3)	½
B40	4*h*	0.325(3)	0.126(3)	½
B41	4*h*	0.373(3)	0.041(3)	½
B42	4*h*	0.490(3)	0.213(3)	½
B4	8*i*	0.066(1)	0.076(1)	0.306(2)
B5	8*i*	0.080(2)	0.174(1)	0.307(3)
B8	8*i*	0.167(3)	0.114(2)	0.308(3)
B9	8*i*	0.171(2)	0.201(2)	0.412(2)
B31	8*i*	0.496(2)	0.369(2)	0.409(3)
B32	4*h*	0.034(3)	0.037(3)	½
B34	4*h*	0.061[b]	0.211[b]	½
B38	4*h*	0.219[b]	0.111[b]	½
B02	8*i*	0.141(2)	0.029(2)	0.407(3)
B10	8*i*	0.217(2)	0.328(2)	0.191(3)
B11	8*i*	0.229(2)	0.383(2)	0.356(3)
B13	8*i*	0.242(2)	0.279(2)	0.331(3)
B14	8*i*	0.273(2)	0.428(2)	0.184(3)
B16	8*i*	0.288(2)	0.264(2)	0.179(3)
B18	8*i*	0.302(2)	0.350(1)	0.085(3)
B19	8*i*	0.329(1)	0.434(1)	0.337(2)
B21	8*i*	0.348(2)	0.265(1)	0.326(2)
B22	8*i*	0.370(1)	0.403(1)	0.177(2)
B23	8*i*	0.380(2)	0.309(1)	0.174(2)
B26	8*i*	0.406(2)	0.357(1)	0.338(2)
B01	8*i*	0.315(2)	0.344(1)	0.415[b]
B45	4*g*	0.051(3)	0.476(3)	0
B48	4*g*	0.100(7)	0.123(7)	0
B55	4*g*	0.433[b]	0.336[b]	0
B56	4*g*	0.374[b]	0.232[b]	0
B35	4*h*	0.139(4)	0.370(3)	½
B36	4*h*	0.188(4)	0.281(3)	½
B37	4*h*	0.191(3)	0.458(4)	½
B39	4*h*	0.298(3)	0.480(3)	½

[a] refined occupancies of Yb1 and polyhedral boron atoms did not deviate from unity; Occ. (B45)=1.0(1); Occ. (B48)=0.32(2); Occ. (B55)=0.32(3); Occ. (B56)=0.28(3); Occ. (B35)=0.92(3); Occ. (B36)=0.86(3); Occ. (B37)=0.92(3); Occ. (B39)=0.98(3); B_{iso} (Yb1)=0.69(1); Isotropic displacement parameters of boron atoms were fixed to 0.8; [b] fixed value

4. Summary

Two boron rich phases in the Yb-B system have been synthesised by borothermal reduction of Yb oxide under vacuum and their crystal structures have been determined by single crystal and/or powder X-ray diffraction. A new YB_{50}-type phase was obtained in single phase conditions at a composition of $YbB_{43.3}$ (Rietveld refinement, powder XPD data) upon annealing at 1500 °C. It decomposes at higher reaction temperatures to the YB_{66}-type compound and an unknown phase. For the former, the structure details were elucidated for the ytterbium-rich $YbB_{56.0}$ composition from single crystal XRD of the specimen annealed at 1825 °C. The upper limit of boron content at this temperature was evaluated as $YbB_{60.4}$ from powder XRD of the sample containing a minor quantity of *β-rh* boron. The solubility of Yb in *β-rh* boron at 1825 °C was found to be very small (~0.72 at.% Yb); ytterbium partially occupies the D and E voids in the structure of *β-rh* boron. The structure analysis showed that basic icosahedral frameworks of $YbB_{43.3}$ and $YbB_{56.0}$ do not change significantly from those of yttrium prototypes, however display certain contractions of inter- and intra-icosahedral bonds. In $YbB_{56.0}$, the Yb is found in a split 48*f* (*x*,¼,¼) atom position with a total occupancy of about 58.5% while for $YbB_{43.3}$ a complete Yb site occupation was found. To our knowledge, this is the first detailed single crystal structural investigation of a heavy rare earth phase of the YB_{66}-type.

Acknowledgements

The research work of O.S. was supported by Austrian FWF project V279-N19. L.S. is grateful to ÖAD for a research fellowship. T.M. thanks JST CREST JPMJCR15Q6.

References

[1] A. U. Seybolt, An exploration of high boron alloys. Trans. Am. Soc. Met. 52 (1960) 971-989.

[2] S.M. Richards, J.S. Kasper, Acta Cryst. 25 (1969) 237–251.

[3] G.A. Slack, D.W. Oliver, G.D. Brower, J.D. Young, J. Phys. Chem. Solids 38 (1977) 45–49.

[4] K. Kamimura, T. Tanaka, S. Otani, Y. Ishizawa, Z.U. Rek, J. Wong, J. Cryst. Growth 128 (1993) 429–434.

[5] T. Tanaka, Y. Ishizawa, J. Wong, Z.U. Rek, M. Rowen, F. Schäfers, B.R. Müller, Jpn. J. Appl. Phys. 10 (1994) 110–113.

[6] I. Higashi, K. Kobayashi, T. Tanaka, Y. Ishizawa, J. Solid State Chem. 133 (1997) 16–20.

[7] T. Tanaka, Y. Shi, T. Mori, A. Leithe-Jasper, J. Solid State Chem. 154 (2000), 54-60.

[8] M.A. Hossain, I. Tanaka, T. Tanaka, A.U. Khan, T. Mori, J. Physics Chem. Solids 87 (2015) 221–227.

[9] K. Schwetz, P. Ettmayer, R. Kieffer, A. Lipp, J. Less-Common Met. 26 (1972) 99-104.

[10] J.S. Kasper, J. Less-Common Met. 47 (1976) 17-21.

[11] Mori, T.: In: Gschneidner, K.A. Jr., Bunzli, J.-C., Pecharski, V. (eds.) Handbook on the Physics and Chemistry of Rare Earths, vol. 38, p. 105. North-Holland, Amsterdam (2008)

[12] K.E Spear, G.I. Solovyev, in: Roth, R.S., Schneider, S.J. Jr. (eds.) Solid State Chemistry, NBS Spec. Pub. 364, Proc. 5th Mat. Res. Symp., p. 597. US Dept. of Commerce, Washington (1972).

[13] K. Flachbart, S. Gabani, T. Mori, K. Siemensmeyer, Acta Phys. Polon. A 118 (2010) 875-876.

[14] V.V. Novikov, D.V. Avdashchenko, S.L. Bud'ko, N.V. Mitroshenkov, A.V. Matovnikov, H. Kim, M.A. Tanatar, R. Prozorov, Phil. Mag. 93 (2013) 1110-1123.

[15] T. Mori, T. Tanaka, J. Solid State Chem. 179 (2006) 2889-2894.

[16] A. Sussardi, T. Tanaka, A.U. Khan, L. Schlapbach, T. Mori, J. Materiomics 1 (2015) 196-204.

[17] T. Tanaka, S. Okada, Y. Ishizawa, J. Alloys Compd. 205 (1994) 281-284.

[18] I. Higashi, T. Tanaka, K. Kobayashi, Y. Ishizawa, M. Takami, J. Solid State Chem. 133 (1997) 11-15.

[19] T. Tanaka, S. Okada, Y. Ishizawa, J. Solid State Chem. 133 (1997) 55-58.

[20] T. Mori, F. Zhang, and T. Tanaka, J. Phys.: Condens. Matter, 13 (2001) L423-L430.

[21] F.X. Zhang, F.F. Xu, A. Leithe-Jasper, T. Mori, T. Tanaka, A. Sato, P. Salamakha, Y. Bando, J. Alloys Comp. 337 (2002) 120–127.

[22] V.I. Matkovich, J. Economy, Acta Cryst. B26 (1970) 616.

[23] T.B.Massalski, BinaryAlloyPhaseDiagrams, second ed., ASM International, Materials Park, OH, 1990.

[24] P.K. Smith, P.W. Gilles, J. Inorg. Nucl. Chem. 26 (1964) 1465-1467.

[25] T. Mori, Z. Kristallogr. 221 (2006) 464–471.

[26] J. Rodriguez-Carvajal, Recent Developments of the Program FULLPROF, Commission on Powder Diffraction (IUCr). Newsletter 26 (2001) 12-19.

[27] O. Sologub, L.P. Salamakha, B. Stöger, P.F. Rogl, H. Michor, E. Bauer, J. Alloys Comp. 675 (2016) 99–103.

[28] Bruker Advanced X-ray solutions. APEX2 User Manual. Version 1.22, Bruker AXS Inc., 2004.

[29] Bruker. APEXII, SAINT and SADABS., Bruker Analytical X-ray Instruments Inc.: Madison, Wisconsin, USA, 2008.

[30] P. McArdle, J. Appl. Cryst. 29 (1996) 306.

[31] L.J. Farrugia, J. Appl. Cryst. 32 (1999) 837-838.

[32] G.M. Sheldrick, SHELXS-97, Program for the Solution of Crystal Structures, University of Göttingen, Germany, 1997.

[33] G.M. Sheldrick, G.M. SHELXL-97, Program for Crystal Structure Refinement, University of Göttingen, 1997.

[34] E. Parthe, L.M. Gelato, Acta Cryst. A40 (1984) 169- 183.

[35] T. Tanaka, K. Kamiya, T. Numazawa, A. Sato, S. Takenouchi, Z. Kristallogr. 221 (2006) 472–476.

[36] S.J. La Placa, D. Noonan, B. Post, Acta Cryst. 16 (1963) 1182.

[37] G.A. Slack, C.I. Hejna, M.F. Garbauskas, J.S. Kasper, J. Solid State Chem. 76 (1988) 64-86.